J Antimicrob Chemother 2012; **67**: 1948–1960
doi:10.1093/jac/dks161 Advance Access publication 25 May 2012

Journal of Antimicrobial Chemotherapy

A new *in vivo* model to test anti-tuberculosis drugs using fluorescence imaging

Andrea Zelmer[1]*, Paul Carroll[2], Nuria Andreu[3], Kristine Hagens[4], Jacqueline Mahlo[4], Natalja Redinger[4], Brian D. Robertson[3], Siouxsie Wiles[5,6], Theresa H. Ward[1], Tanya Parish[2,7], Jorge Ripoll[8], Gregory J. Bancroft[1] and Ulrich E. Schaible[1,4]

[1]Immunology and Infection Department, Faculty of Infectious and Tropical Diseases, London School of Hygiene and Tropical Medicine, Keppel St., London WC1E 7HT, UK; [2]Centre for Immunology and Infectious Disease, Barts and The London School of Medicine and Dentistry, Queen Mary University of London, 4 Newark Street, London E1 2AT, UK; [3]Microbiology, Department of Medicine, Imperial College London, South Kensington Campus, London SW7 2AZ, UK; [4]Cellular Microbiology, Department of Molecular Infection Research, Research Centre Borstel, Parkallee 22, 23845 Borstel, Germany; [5]Infectious Diseases & Immunity, Department of Medicine, Imperial College London, Hammersmith Campus, London W12 0NN, UK; [6]Department of Molecular Medicine and Pathology, University of Auckland, 85 Park Rd, Auckland, 1142, New Zealand; [7]Infectious Disease Research Institute, 1124 Columbia St., Seattle, WA 98104, USA; [8]Institute for Electronic Structure and Laser, Foundation for Research and Technology—Hellas, PO Box 1527, 71110 Heraklion, Greece

*Corresponding author. Tel: +442079588269; Fax: +442073235687; E-mail: andrea.zelmer@lshtm.ac.uk

Received 13 January 2012; returned 21 February 2012; revised 3 April 2012; accepted 5 April 2012

Objectives: The current method for testing new drugs against tuberculosis *in vivo* is the enumeration of bacteria in organs by cfu assay. Owing to the slow growth rate of *Mycobacterium tuberculosis* (*Mtb*), these assays can take months to complete. Our aim was to develop a more efficient, fluorescence-based imaging assay to test new antibiotics in a mouse model using *Mtb* reporter strains.

Methods: A commercial IVIS Kinetic® system and a custom-built laser scanning system with fluorescence molecular tomography (FMT) capability were used to detect fluorescent *Mtb* in living mice and lungs *ex vivo*. The resulting images were analysed and the fluorescence was correlated with data from cfu assays.

Results: We have shown that fluorescent *Mtb* can be visualized in the lungs of living mice at a detection limit of $\sim 8 \times 10^7$ cfu/lung, whilst in lungs *ex vivo* a detection limit of $\sim 2 \times 10^5$ cfu/lung was found. These numbers were comparable between the two imaging systems. *Ex vivo* lung fluorescence correlated to numbers of bacteria in tissue, and the effect of treatment of mice with the antibiotic moxifloxacin could be visualized and quantified after only 9 days through fluorescence measurements, and was confirmed by cfu assays.

Conclusions: We have developed a new and efficient method for anti-tuberculosis drug testing *in vivo*, based on fluorescent *Mtb* reporter strains. Using this method instead of, or together with, cfu assays will reduce the time required to assess the preclinical efficacy of new drugs in animal models and enhance the progress of these candidates into clinical trials against human tuberculosis.

Keywords: antibiotics, drug testing, mycobacteria, optical imaging, TB

Introduction

Tuberculosis (TB) is still among the most prevalent infectious diseases worldwide, causing 1.7 million deaths globally in 2009, and is currently estimated to infect one-third of the world's population.[1] Control strategies to prevent further spread of the disease include prompt detection, treatment and prophylactic vaccination. The only vaccine currently available against TB is *Mycobacterium bovis* bacille Calmette–Guérin (BCG), which has been used safely for decades but is not effective against pulmonary TB in tropical countries, and is contraindicated in people infected with HIV.[2,3] Antibiotic treatment is available, but regimens require administration of two or three drugs for 6–9 months, and full completion is necessary to minimize the risk of evolving drug-resistant strains. This requires high patient compliance, and a steady supply of drugs, and the latter cannot always be guaranteed in low-income countries. *Mycobacterium tuberculosis* (*Mtb*) strains resistant to a single drug have

emerged in every country surveyed, and multidrug-resistant strains, defined as strains resistant to at least isoniazid and rifampicin, are prevalent, particularly in Eastern Europe.[1] In addition, 57 countries worldwide had reported at least one case of TB caused by an extensively drug-resistant (XDR) strain, resistant to first- and second-line drugs, by September 2009.[4] The increase in drug resistance and the lack of an effective vaccine against adult TB are serious threats to the control of TB, creating a great need to identify and develop new anti-TB drugs and vaccines.

Preclinical *in vivo* models are needed to test new drugs for both their efficacy and their pharmacodynamics and pharmacokinetics, which cannot be achieved *in vitro*. This is particularly important in TB as immunopathology leads to the formation of granulomatous lesions in patients during the course of the disease.[5,6] These rigid structures are thought to sequestrate the bacilli and prevent spread throughout the body; however, they could also prevent drugs from penetrating into the tissue and reaching the target bacteria. Mouse models of TB are well established and provide suitable and convenient tools for early stage drug screening, although the lesions formed in the mouse lung can differ from those in TB patients.[7,8] However, pathology still occurs and can lead to gross changes in the tissue morphology of the infected mouse lung.[9,10] Another fact that needs to be considered when testing new drugs is that mycobacteria can alter their metabolic state during growth and persistence inside the host tissue and can switch to a less active or dormant state in which they may become less susceptible to antibiotics.[11] Different mouse models of TB exist which resemble certain aspects of human TB, including those for granuloma necrosis and hypoxia in C3HeB/FeJ mice, a variety of models for chronic or latent infection, as well as for active progressive infection in the absence of adaptive immunity in severe combined immunodeficiency (SCID) mice.[9,12]

To assess the efficacy of a new anti-TB drug in mice, bacterial viability and growth has been measured to date by cfu assays in target organs such as the lung and spleen. This method is reliable and accurate, but it is time-consuming and labour-intensive and provides only retrospective data, as mycobacterial colonies can take up to 6 weeks to become countable. Moreover, cfu assays are endpoint measurements, which require killing the animal. This not only increases the number of animals required and the cost, thereby decreasing the number of drug candidates that can be screened at any one time within the limited aerosol containment space available at most animal facilities, but also prohibits a further follow-up of an individual animal for long-lasting drug effects or remission. In contrast, biophotonic imaging (BPI) of bioluminescent or fluorescently labelled bacteria would enable an instant assessment of bacterial load and location by using highly sensitive cameras to directly measure the visible light produced by these microorganisms. By utilizing labelled strains that maintain the virulent traits of the parental *Mtb* strain in a mouse infection model, this should help to speed up the process of drug screening. It would allow longitudinal studies in which individual animals can be followed over time, and therefore helping to reduce the number of animals needed and to decrease the variation in the data.[13–17] BPI has been used extensively to monitor the progression of other bacterial infections, bacterial gene expression and the effect of vaccines or drugs.[18] Although bioluminescence was used in the majority of these studies, both methods have their advantages and disadvantages. Bioluminescence provides a superior signal-to-noise ratio and, due to its enzymatic nature, allows the rapid detection of changes in microbial metabolism.[19] In contrast, fluorescent proteins (FPs) do not rely on co-factors or administration of an exogenous substrate (which may be subject to tissue penetration issues), bacterial colonies are often characterized by a coloured appearance,[20] which is a convenient indicator of marker protein expression, and results obtained by *in vivo* imaging can easily be followed up by fluorescence microscopy once animals are killed. Absorption and consequently penetration of light through tissue is a challenging issue for *in vivo* imaging approaches. Absorption of light is dependent on wavelength and tissue type. Light of longer wavelengths travels better through tissue, and blood-rich tissue absorbs light more efficiently than less vascularized tissue. Importantly, absorption drops rapidly between the wavelengths of ~580 and ~650 nm.[21] Therefore, the use of red FPs is favoured for *in vivo* imaging over green or yellow FPs, but often green FP (GFP) is the reporter of choice, whereas the use of red FPs (RFPs) for infectious disease models is still rare.[18] The red fluorescent reporter strains of *Mtb* in combination with the instrumentation described in this study are expected to allow visualization of fluorescent signals up to 0.5 cm deep in lung tissue.

The purpose of this study was to develop a fluorescence-based imaging assay using reporter strains of *Mtb* to expedite and facilitate *in vivo* testing of anti-TB drugs. We have previously described the development of *Mtb* strains expressing RFPs.[20] Here we characterized these fluorescent strains for *in vivo* and *ex vivo* imaging in an immune-compromised mouse model of infection, which allows the progressive growth of *Mtb*, using a commercially available IVIS Kinetic® system to provide proof of principle that fluorescence imaging can be employed to evaluate the efficacy of new anti-TB drugs *in vivo*. To verify IVIS results and improve the resolution of images, we used a custom-built laser scanning (LS) system. Our aim was to assess the feasibility and sensitivity of fluorescence imaging for monitoring the course of *Mtb* infection in mice and the impact of antibiotic treatment on bacterial burden.

Materials and methods

Bacterial strains and culture conditions

Bacterial strains, plasmids and FPs used in this study are summarized in Table 1. Construction of reporter plasmids was described previously in detail.[20] Briefly, the promoter P_{smyc} was amplified by PCR from pSE100 and cloned into the vector pSMT3 to generate pSMT3-S via BamHI/XbaI restriction sites.[22,23] In the case of pCherry10, the G13 promoter from *Mycobacterium marinum* was used to generate pSMT3-G13. mCherry, tdTomato and Turbo-635 sequences were codon-optimized for *Mtb* codon preferences, synthesized (Genscript USA Inc., Piscataway, USA) and cloned into pSMT3-S via BamHI/HindIII restriction sites to generate pCherry3, pAsta3 and pCharge3, respectively. mCherry was cloned into pSMT3-G13 via BamHI/HindIII restriction sites to generate pCherry10. Subsequently plasmids were electroporated into the *Mtb* H37Rv parental strain (ATCC 25618) as described previously.[20,22,24]

Mtb wild-type (WT) strain H37Rv and its fluorescent derivatives Charge3, Cherry3, Cherry10 and Asta3 were cultured in Middlebrook 7H9 medium (Sigma-Aldrich, Taufkirchen, Germany) containing 10% Middlebrook OADC (oleic acid, albumin, dextrose, catalase) supplement (BD, Heidelberg, Germany) and 0.5% glycerol (Sigma-Aldrich) without

Table 1. Summary of bacterial strains used in this study, as described previously[20]

Strain	FP expressed	Plasmid	Quantum yield of FP	Excitation coefficient of FP (M^{-1} cm^{-1})	Brightness of FP (% of DsRed)	λ of FP (nm)[a]	
						ex	em
H37Rv	none	NA	NA	NA	NA	NA	NA
Cherry3	mCherry[26]	pCherry3 (P_{smyc} promoter; Addgene plasmid 24659)	0.22	72000	27	587	610
Cherry10	mCherry[26]	pCherry10, (G13 promoter; Addgene plasmid 24664)	0.22	72000	27	587	610
Charge3	Turbo-635[27]	pCharge3(P_{smyc} promoter; Addgene plasmid 24658)	0.34	65000	37	588	635
Asta3	tdTomato[26]	pAsta3 (P_{smyc} promoter; Addgene plasmid 24657)	0.69	138000	160	554	581

λ, wavelength; NA, not applicable.
[a]Wavelengths are represented by maxima of excitation (ex) and emission (em) spectra.

agitation or on Middlebrook 7H11 agar plates (BD) containing 10% Middlebrook OADC supplement and 0.5% glycerol. Hygromycin B (100 mg/L; Sigma-Aldrich, Gillingham, UK) was added to the culture media or plates when required, as described previously.[20] Bacterial cultures were washed once with 1×PBS, resuspended in 1×PBS + 10% glycerol, aliquoted, frozen and stored at −80°C for later use. The number of viable bacteria in frozen stocks was determined by plating a series of 10-fold dilutions on 7H11 agar plates and enumeration of colonies after 4–6 weeks of incubation at 37°C. To prepare the inocula for infection of mice, bacteria were thawed, washed once with 1×PBS and resuspended in 1×PBS to the required concentration.

Infection of animals

All experiments were performed in accordance with the German Animal Protection Law and under ABSL3 aerosol containment. Animal experiments were approved by the Ethics Committee for Animal Experiments of the Ministry for Agriculture, Environment, and Rural Areas of the State of Schleswig-Holstein (Kommission für Tierversuche/Ethik-Kommission des Landes Schleswig-Holstein) under the licenses 13–2/10 ('Analyse von Reporterstämmen des Tuberkuloseerregers'/'Analysis of reporter strains of the causative agent of tuberculosis') and 39–4/11 ('Testung von Moxifloxacin gegen Tuberkulose mittels *in vivo* Imaging'/'Testing of moxifloxacin against tuberculosis by *in vivo* imaging').

Six- to 12-week-old CB-17 SCID mice or SCID Hairless Outbred (SHO) mice (Charles River, Germany) were anaesthetized with a ketamine (125 mg/kg, WDT, Garbsen, Germany) and Rompun (2.5 mg/kg, active ingredient xylazine; Bayer, Leverkusen, Germany) solution by intraperitoneal injection, and infected with parental *Mtb* H37Rv or its fluorescent derivatives in 20 μL of PBS via the intranasal route, with inocula as indicated in the figure legends. The input inocula were confirmed by plating 10-fold dilutions onto 7H11 agar plates containing 10% OADC supplement and 0.5% glycerol, and incubating for 6 weeks at 37°C.

Moxifloxacin treatment

To prepare the moxifloxacin solution, 20% Captisol (w/v; Cydex Pharma, Lenaxa, USA) was dissolved in water. Moxifloxacin (Apin Chemicals Limited, Abingdon, UK) was then added to a final concentration of 5000 mg/L and the solution was sterile filtered. Mice were given seven daily doses of 50 mg/kg body weight of moxifloxacin by oral gavage, starting 1 day after infection.

Imaging of animals and organs

All imaging was performed in an ABSL3 aerosol containment laboratory in accordance with local safety regulations.

To increase the signal-to-noise ratio in animals used for imaging, fur was removed from the thoracic area approximately once a week. The mice were anaesthetized with a ketamine and xylazine solution by intraperitoneal injection as described above. Once fully unconscious, a depilating cream (Veet, Slough, UK) was applied and left for ∼5 min. The cream was then removed with soft tissue paper to minimize skin irritation and the area cleaned with water and soft tissue paper to avoid non-specific fluorescence from residual cream.

On all other occasions when imaging was performed, mice were anaesthetized with 4% isoflurane gas (Actavis, Munich, Germany) and, once inside the camera chamber, anaesthesia was maintained by administering 2%–3% isoflurane through individual nose cones.

Imaging of live animals or organs was performed using either an IVIS Kinetic® imaging system (Caliper Life Sciences, Preston Brook Runcorn, UK) or a custom-built LS system. The IVIS system consisted of a cooled charge-coupled device (CCD) camera mounted onto a light-tight specimen chamber. The fluorescent excitation light was provided by a halogen lamp in combination with appropriate excitation filters. Emission filters were placed in front of the camera aperture to allow recording of specific wavelengths of light, depending on the emission spectra of the FP examined. Non-specific fluorescence was recorded by using a lower wavelength excitation filter and subtracted from original images by using the Image Math Tool in Living Image software (version 3.2, Caliper Life Sciences). The corrected image was then superimposed onto a greyscale reference photograph taken under low illumination using the Living Image software to aid the determination of the anatomical location of the signal. Fluorescence was quantified on the raw data before non-specific fluorescence was removed, by using the Region of Interest (ROI) tool in the Living Image software, where only light emanating from within a specified area was measured. Images were acquired using the following settings unless otherwise stated: excitation filter 605 nm and emission filter 660 nm (Charge3, Cherry3, Cherry10) or excitation filter 570 nm and emission filter 620 nm (Asta3); background excitation filter 465 nm; f-stop 1.2; binning 4; exposure time 3–10 s. Fluorescence intensity was displayed on a pseudocolour spectrum (where dark red represents the lowest intensity and yellow the highest) and presented as efficiency, a measurement normalized to the incident excitation intensity (efficiency = radiance of the subject/illumination intensity). By displaying fluorescence as efficiency, images taken at different timepoints and with different exposure times could be directly compared with each other.

The LS system comprised a similar configuration, with a CCD camera (iKonM; Andor Technology, Belfast, Northern Ireland) placed on top of a light-tight specimen chamber and emission filters in front of the camera aperture. The fluorescent excitation light was provided by a 593 nm laser (RGBLase LLC, Fremont, California, USA), which was guided onto the specimen by several mirrors. Fine movement of the laser beam was controlled by a Scancube®7 scan head (Scanlab,

Puchheim/Munich, Germany). To acquire fluorescence images, the laser was scanned across the whole specimen in one motion and a single image was acquired using a specific emission filter to capture the total fluorescence emission (centre wavelength 620 nm/bandwidth 40 nm or centre wavelength 650 nm/bandwidth 60 nm; Chroma Technology, Bellow Falls, Vermont, USA). The emission filter was then removed and another image was acquired in the same way to yield an excitation image. The fluorescence intensity was normalized by the median excitation intensity across the image using Matlab software [version 7.7.0.471 (R2008b); MathWorks, Cambridge, UK], and the normalized fluorescence image was superimposed onto a greyscale reference photograph. Images were acquired with an exposure time of 2–3 s. Fluorescence was quantified using ROI analysis. Fluorescence intensity was displayed on a pseudocolour spectrum (where blue represents the lowest intensity and yellow the highest) and presented as normalized fluorescence so that images acquired with different exposure settings could be compared directly.

When organs were imaged, they were placed as flatly as possible to allow full and consistent light penetration in order to minimize potential variation in the measurements due to different tissue thickness.

Enumeration of bacteria in tissues

At the specified timepoints, animals were killed by cervical dislocation whilst under anaesthesia. Lungs and spleens were removed aseptically and homogenized by mechanical disruption in sterile WTA buffer consisting of 1% (w/v) BSA (Serva, Heidelberg, Germany), 1% (v/v) Tween 80 (Sigma-Aldrich) in sterile water. A cfu assay was performed by plating a series of 10-fold dilutions of tissue homogenates onto 7H11 agar plates with 10% OADC supplement and 0.5% glycerol. Bacteria were grown on non-selective media to determine the stability of FP expression by evaluating colony colour. Plates were incubated at 37°C and colonies counted after 8–12 weeks.

Statistical analysis

Statistical analysis was performed using GraphPad Prism version 4.02. To compare fluorescence efficiencies or cfu burden between mice infected with *Mtb* H37Rv WT or *Mtb* Charge3, a Mann–Whitney test was used. For cfu, groups of five mice were compared. Where more than two groups were compared, a Kruskal–Wallis test with Dunn's post test for multiple comparisons was performed. For analyses of *in vivo* fluorescence efficiency, all animals were included in each analysis. To test the correlation of cfu burden and fluorescent signal, a Pearson correlation test was performed. Linear regression analysis was used to determine the relationship between cfu and fluorescence.

Results

Red fluorescent proteins are stably expressed in M. tuberculosis and do not attenuate growth in vivo

Light of longer wavelengths is better suited for *in vivo* imaging than light of shorter wavelengths, because it penetrates deeper into the tissue and causes less autofluorescence.[25] We therefore chose to investigate *Mtb* strains expressing the RFPs mCherry (designated Cherry3 and Cherry10), Turbo-635 (designated Charge3) or tdTomato (designated Asta3) for their suitability for *in vivo* imaging (see Table 1).[26,27] We have previously shown that these strains express the marker proteins stably and at high levels *in vitro*.[20] Since the expression of exogenous proteins often places a metabolic burden on the bacterial cell, which can cause attenuation of virulence, we first compared the virulence of these strains against the parental WT strain H37Rv. CB-17 SCID mice were infected with H37Rv WT or fluorescent reporter strains via the intranasal route and the number of bacteria in lungs and spleens was determined by cfu assay of organ homogenates during the course of infection (Figure 1). After 5 days, comparable numbers of WT, Charge3, Cherry10 and Asta3 bacteria ($\sim 10^5$–10^6 cfu) were detected in lungs of CB-17 SCID mice, whilst Cherry3 had grown significantly less than the other strains (difference compared with Cherry3: H37Rv, 38-fold, $P<0.05$; Charge3, 27-fold, $P>0.05$; Cherry10, 51-fold, $P<0.01$; Figure 1a), but this difference was absent at day 20 after infection, when all fluorescent strains had reached higher mean lung cfu values than the WT (Figure 1b). Bacteria of all tested strains were found to spread to the spleen at a later timepoint of infection, and the bacterial burden of fluorescent strains was similar or higher than the WT (Figure 1c). From these data we conclude that the expression of these RFPs did not attenuate *in vivo* virulence of *Mtb*.

Fluorescent M. tuberculosis can be detected in mouse lungs in vivo

To establish whether growth of the reporter strains could be visualized *in vivo*, the CB-17 SCID mice infected above (Figure 1) were imaged at day 16 or 20 after infection using an IVIS imaging system before being killed for cfu enumeration. On day 20, specific fluorescent signals were detected in the thoracic area of four out of five mice infected with *Mtb* Charge3, whilst weak signals were found in two out of five mice infected with *Mtb* Cherry3, and no signal was observed in mice infected with *Mtb* Cherry10 or Asta3 (Figure 2). Mice infected with *Mtb* H37Rv WT were imaged under the same conditions and served as a negative control. No specific fluorescent signals were detected in the thoracic area of these animals. Non-specific fluorescence was detected in the abdominal area of some animals, which most likely originated from food in the stomach and intestinal tract. As the bacterial burden in the lungs of infected animals was comparable between the different reporter strains (Figure 1) and *Mtb* Charge3 produced the strongest fluorescent signal (Figure 2), this strain was selected for further studies.

To further analyse the kinetics of infection and the limit of bacterial detection, CB-17 SCID mice were infected intranasally with *Mtb* Charge3, images were acquired on the IVIS system at 1, 7, 12 and 15 days post-infection, and bacterial loads in lungs and spleens were determined by cfu assay (Figure 3). Fluorescence was quantified by ROI analysis in the Living Image software over the thoracic area on raw data before non-specific background was subtracted. One group of mice was infected with *Mtb* H37Rv WT and served as a negative control for fluorescence imaging. The bacterial burden in lungs and spleens increased steadily over time, reaching 4×10^7–2.3×10^8 cfu/lung of *Mtb* Charge3 on day 15 (Figure 3b). Bacteria could be cultured from spleens of all animals from day 13 onwards, reaching a peak of 6×10^3–5.5×10^4 cfu/spleen at day 15 (Figure 3c). Accordingly, the fluorescent signal emanating from the thoracic area also increased over time in mice infected with *Mtb* Charge3 such that on days 12 and 15 after infection *Mtb* Charge3-infected mice displayed significantly higher fluorescence than mice infected with *Mtb* H37Rv WT ($P=0.0043$ and $P=0.0020$,

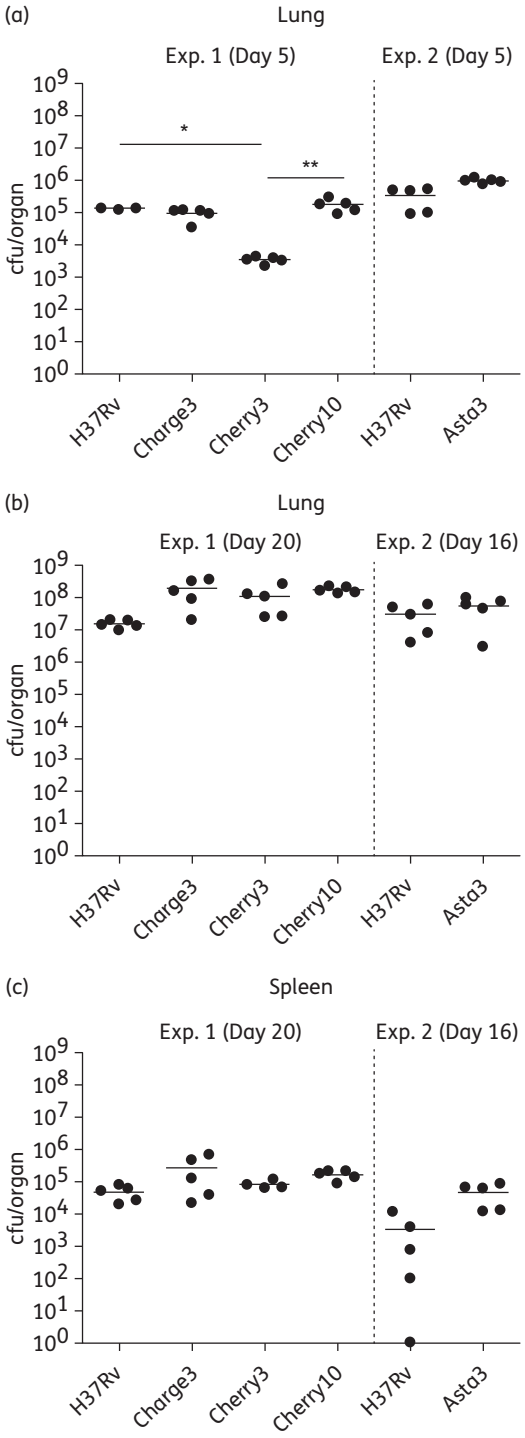

Figure 1. Fitness testing of fluorescent reporter strains of *Mtb*. In two separate experiments (Exp. 1 and Exp. 2) CB-17 SCID mice ($n=5$) were infected with fluorescent or WT strains of *Mtb* via the intranasal route. (a) cfu in lung tissue at the early timepoint (5 days after infection). (b) cfu in lung tissue at later timepoints (16 and 20 days after infection). (c) cfu in spleen tissue at later timepoints (16 and 20 days after infection). Each data point represents an individual organ, and horizontal lines represent the means. Input inocula/mouse: Exp. 1: H37Rv, 2.9×10^3 cfu; Charge3, 1.2×10^3 cfu; Cherry3, 2×10^3 cfu; Cherry10, 2.3×10^3 cfu; Exp. 2: H37Rv, 1×10^4 cfu; Asta3, 4×10^3 cfu. $^{**}P<0.01$; $^{*}P<0.05$.

respectively; Figure 3a and d). It should be noted that Figure 3(a) depicts one representative group of mice to allow comparison of the same group of five animals over time, whilst Figure 3(d) shows the average fluorescence measured in all animals still in the experiment at the respective timepoints. Therefore, fluorescence levels differ between Figure 3(a) and Figure 3(d). Images of the groups of mice used for determination of cfu are shown in Figure S1 (available as Supplementary data at *JAC* Online). The fold increase in fluorescence in *Mtb* Charge3-infected mice over the mice infected with the non-fluorescent *Mtb* H37Rv WT was comparable on days 12 and 15 after infection (Figure 3d; 1.30-fold and 1.34-fold, respectively), which is in accordance with the cfu data (Figure 3b). There was no detectable signal in the spleen area, which was most likely due to the lower numbers of bacteria present in this organ. Based on the observation that a specific signal was first evident on day 12 after infection (Figure 3a and d), we estimate the detection limit of *Mtb* Charge3 *in vivo* to be 8×10^7 cfu/lung.

Stability of FP expression was analysed for *Mtb* Charge3 at each timepoint when cfu were determined, by visually scoring whether bacterial colonies were coloured or not (Table 2). More than 90% of bacteria expressed the FP throughout the course of the infection, in both lung and spleen tissues, indicating that the reporter plasmid was stably maintained in the bacteria during the infection.

Imaging of lung tissue ex vivo

To test whether imaging of infected lungs *ex vivo* could also provide a rapid way to assess bacterial burden, all lungs harvested during the experiment described in Figure 3 were imaged using the IVIS system before processing for cfu (Figure 4). Fluorescence was quantified by ROI analysis (Living Image software) and increased steadily over time in accordance with cfu data (Figure 4b). A first signal could be detected in one lung infected with *Mtb* Charge3 on day 7. Stronger specific signals were detected in all lungs on days 13 and 15 after infection with *Mtb* Charge3, whilst lungs infected with *Mtb* H37Rv WT did not show any specific fluorescent signal (Figure 4a). The measured fluorescence correlated well with the bacterial load in each organ ($r=0.7564$, $P=0.0011$; Figure 4c). A linear regression analysis was performed to calculate the detection limit of this assay (Figure 4c). Based on the notion that any detectable amount of reporter bacteria should emanate higher amounts of fluorescence than WT bacteria, Y was set based on the average amount of fluorescence detected in the five *Mtb* H37Rv WT-infected lungs. The average fluorescence measured was 3.2×10^{-5}, and the threshold for the background signal (Y) was arbitrarily set to 3.5×10^{-5}. From this, the detection limit for the excised organ was calculated as 1.1×10^7 cfu/lung.

To further improve the sensitivity, as well as resolution of the fluorescent signal, we employed a custom-built LS system, where the laser scans across the whole organ and captures the emitted light in a single image. To test whether this system improved upon the IVIS imaging, excised lungs from CB-17 SCID mice infected with *Mtb* Charge3, or *Mtb* H37Rv WT-infected lungs as negative controls, were imaged (Figure 5). Mice were killed on day 12, 15 or 18 after infection, their lungs aseptically removed and images of all lungs acquired on both systems. To demonstrate the range of signals measured, three lungs with

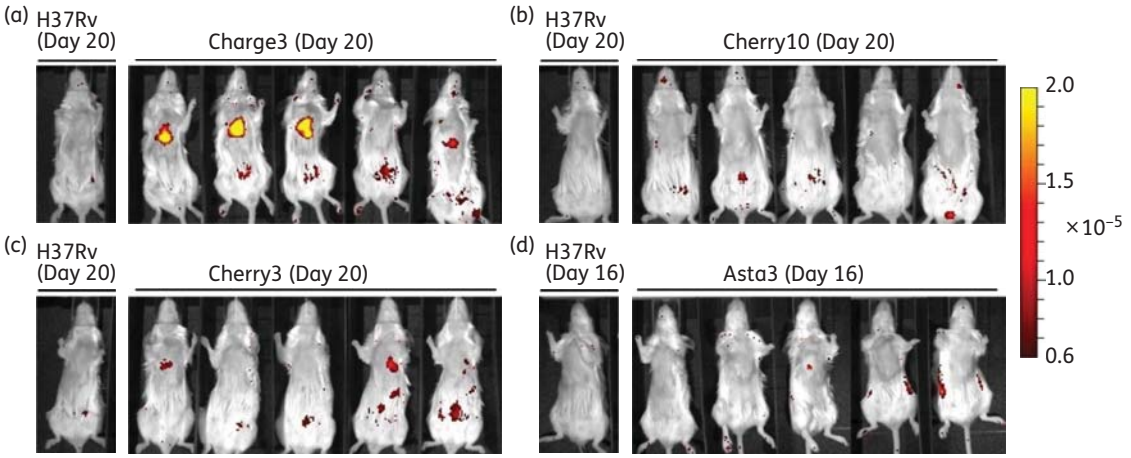

Figure 2. *In vivo* imaging of *Mtb* reporter strains. CB-17 SCID mice infected in Figure 1 with *Mtb* Charge3, Cherry3, Cherry10, Asta3 or the parental *Mtb* H37Rv WT strain were imaged using the IVIS system at 16 days (d) or 20 days (a–c) post-infection. Images were taken using the following settings: (a–c) excitation filter 605 nm, emission filter 660 nm, f-stop 2, exposure time 3 s; (d) excitation filter 570 nm, emission filter 620 nm, f-stop 2, exposure time 5 s. Non-specific fluorescence was recorded using a lower excitation wavelength [(a–c) 500 nm; (d) 465 nm]. Fluorescence intensity is presented as efficiency and depicted as false colour, where dark red corresponds to the lowest intensity and yellow to the highest intensity.

low and three with high fluorescent signals are shown, with IVIS images shown in the top row and corresponding LS images of the same lung shown underneath (Figure 5a). The images taken with the LS system showed clearly superior resolution of the fluorescent signal when compared with the IVIS images. However, a difference in fluorescence intensity was not observed between the two systems, suggesting comparable sensitivity of both approaches with our current set-up.

Ex vivo imaging for drug efficacy testing

Since *ex vivo* imaging of infected lungs using the IVIS system proved to be a viable method to assess bacterial burden as an alternative to cfu assays, we tested whether this was also true for the LS system, and whether both approaches could be used to document the effect of antibiotic treatment, providing a faster, more efficient way to test new anti-TB drugs. SHO mice were infected intranasally with *Mtb* Charge3 and given daily doses of moxifloxacin (50 mg/kg body weight) or saline by oral gavage on days 1–7 after infection. One group of mice was infected with *Mtb* H37Rv WT as negative control for imaging and was given saline by oral gavage together with the rest of the mice. For each timepoint (on day 1 before treatment was started and on days 9, 19 and 28 after infection), lungs were aseptically removed and imaged in both IVIS and LS systems before processing for cfu (Figures 6 and 7).

A specific signal was detected as early as day 9 in lungs from saline-treated infected mice, and ROI analysis showed a 1.37-fold increase in fluorescence over the signals measured in lungs from moxifloxacin-treated mice using the IVIS system and a 2.07-fold increase using the LS system ($P=0.0079$ for both; Figure 6). Fluorescence increased steadily over time in the saline-treated group up to day 28. In the moxifloxacin-treated group, fluorescence was lower than in the saline group on day 19 (2.89-fold for IVIS and 3.99-fold for LS) and day 28 (1.41-fold for IVIS and 2.33-fold for LS), but the difference was only significant on day 19 ($P=0.0159$ for both; Figure 6b and c). Bacterial burden in the lungs as assessed by cfu assay increased over time in the saline-treated group, but dropped slightly up to day 19 in the moxifloxacin-treated group (2.3-fold decrease from day 1 to day 19; Figure 7a) with a significant difference between the two groups on days 9 and 19 ($P=0.0079$ and $P=0.0159$, respectively), but not on day 28 ($P=0.4206$). Data from the saline group of this experiment were used to correlate cfu to the fluorescent signals measured by either of the two imaging systems (Figure 7b and c). Better correlation was achieved when using the LS system compared with the IVIS system, although in both cases the correlation was highly significant ($r=0.9223$, $P<0.0001$ and $r=0.7992$, $P<0.0001$, respectively). Linear regression analysis was used to calculate the detection limit of this assay (Figure 7b and c). Y was set based on the average amount of fluorescence detected in *Mtb* H37Rv WT-infected lungs on day 28. The measured average fluorescence ($n=5$) was 8.99×10^{-6} for the IVIS system and 351.9 for the LS system, and the threshold for the background signal (Y) was arbitrarily set to 1×10^{-5} and 400, respectively. Using these values, the detection limit was calculated as 5.90×10^{4} cfu/lung for the IVIS system and 7.51×10^{4} cfu/lung for the LS system, providing ~1000-fold improvement over the *in vivo* method and corroborating comparable sensitivity of the two imaging systems.

Discussion

Here we provide the first known report of detection of *Mtb* in live animals by fluorescence non-invasive imaging during progressive infection. We investigated the suitability for *in vivo* imaging of four different red fluorescent *Mtb* reporter strains, and found that all strains retained virulence when compared with the parental H37Rv WT strain despite the expression of plasmid-encoded FPs. While mean bacterial burdens were comparable between all strains at day 20 post-infection, we observed a strong fluorescent signal only from mice infected with the Charge3 strain. Better detectability over other reporter strains is

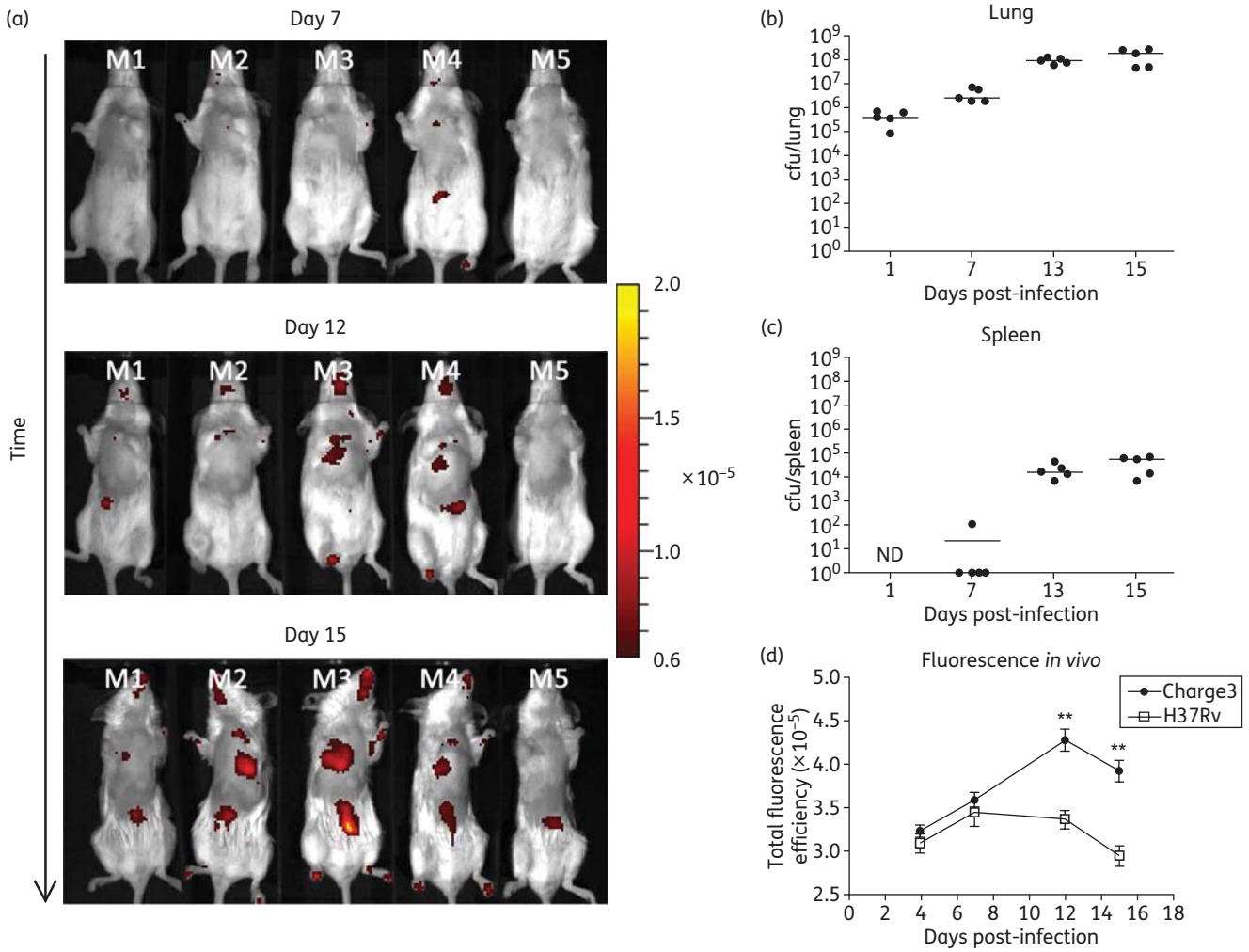

Figure 3. Time course of infection of CB-17 SCID mice with *Mtb* Charge3. Groups of CB-17 SCID mice ($n=5$/group) were infected via the intranasal route with *Mtb* Charge3 or the parental *Mtb* H37Rv WT strain. (a) The same representative group of five animals (indicated by M1–M5) is shown in each image. Images were acquired at the indicated timepoints with an exposure time of 10 s. Fluorescence intensity is presented as efficiency and depicted as false colour, where dark red corresponds to the lowest intensity and yellow to the highest intensity. (b) and (c) Bacterial burden of *Mtb* Charge3 as cfu in lung and spleen, respectively, over the course of the infection. Each data point represents an individual organ, and horizontal lines represent the means. (d) Quantification of fluorescence intensity over the thoracic area only as determined by ROI analysis. All animals were included in this analysis up to the timepoint when they were killed for cfu analysis or because they had reached their humane endpoint (Charge3 infected: $n=25$ for days 4 and 7; $n=20$ for day 12; $n=15$ for day 15; H37Rv infected: $n=5$ for all timepoints). Data are presented as means ± SEM (Charge3, filled circles; H37Rv, open squares). Due to logistical constraints within the containment suite, images were acquired on day 12 after infection, whilst bacterial burden was determined the following day (day 13). Input inocula/mouse: Charge3, 1.7×10^4 cfu; H37Rv, 2×10^3 cfu. $^{**}P<0.01$. ND, not determined.

most likely due to the following two factors. Firstly, absorption of light by tissue depends on the wavelength and declines rapidly between ~580 and ~650 nm.[21] Therefore, a difference of 25 nm in the maximum emission wavelength (i.e. a shift from 610 to 635 nm between mCherry and Turbo-635, respectively) will have a considerable impact on signal detection *in vivo*. Secondly, *Mtb* Charge3 was previously found to be brighter than *Mtb* Cherry3 and *Mtb* Asta3 in liquid cultures *in vitro*.[20] Based on the high level of fluorescence observed after *in vivo* imaging, Charge3 was chosen for further studies. We were able to visualize ~8×10^7 bacteria of *Mtb* Charge3 in the lungs of living animals from day 12 to day 15 after infection. This is based on detection of the first specific signal on day 12 after infection. Specificity was defined as the significant increase in fluorescence in *Mtb* Charge3-infected mice over *Mtb* H37Rv WT-infected controls. We observed some variation of background fluorescence over time in whole *Mtb* H37Rv WT-infected animals. Therefore, we recommend the inclusion of a control group of mice infected with non-fluorescent bacteria at each timepoint of imaging. Importantly, *Mtb* Charge3 maintained stable expression of the reporter FP during the entire course of infection, as indicated by the colour of colonies grown in cfu assays. This method could therefore be useful for high-dose models of acute *Mtb* infection employed in drug testing or therapeutic vaccine studies.

Table 2. Stability of marker protein expression in *Mtb* Charge3

	Lungs		Spleen	
Time (days)	% coloured (mean)	SD	% coloured (mean)	SD
1	91.4	5.47	ND	ND
7	94.8	2.91	ND	ND
13	93.1	3.11	91.0	6.67
15	93.3	2.96	94.2	5.95

ND, not determined.
The mean percentage of red-coloured colonies recovered from lung or spleen tissue from CB-17 SCID mice at indicated timepoints after infection is shown. The mean and SD were calculated from organs of five individual mice per timepoint.

A previous report has described imaging in the lungs of living mice of an *M. bovis* BCG vaccine strain expressing tdTomato, but animals were imaged immediately after infection, not allowing time for the infection to evolve naturally.[28] More recently, the same group developed a new method where fluorescence emitted from a reporter enzyme reaction is measured. Using this method, they were able to detect as few as 10^4 cfu BCG and 10^6 cfu *Mtb* in the lungs of living mice when substrate was given immediately after infection.[29] The authors also report a significant difference in fluorescent signal after 6 days of treatment with isoniazid and rifampicin in mice infected with 10^6 cfu *Mtb*. However, this technique requires the administration of exogenous fluorogenic substrate 24–48 h before imaging, whilst in our system imaging can be performed at any time, independently of exogenous substrate administration.

Where the detection of lower numbers of bacteria is desirable, an *ex vivo* approach represents a useful alternative to *in vivo* imaging. This is still an endpoint method where the animal has to be killed, but allows instant assessment of bacterial load and location and of the effect of a new drug or vaccine without the additional 4–6 weeks needed for cfu assays. In this way, informed decisions regarding the infection status of the remaining animals can be made immediately during the course of an experiment, e.g. whether treatment should be initiated or delayed until a certain bacterial burden is reached. Using two different imaging systems we have shown that the bacterial burden correlates to the fluorescent signals measured in excised lungs. A high-dose infection led to a high bacterial burden in the lungs of CB-17 SCID mice, accompanied by macroscopically visible changes in lung morphology with a highly congested and inflamed appearance on days 12 and 15 after infection (data not shown). The onset of weight loss in animals (data not shown) was observed within 2 weeks after infection, and a detection limit for *ex vivo* lung imaging of 1.1×10^7 cfu was found. In an attempt to increase sensitivity *in vivo* by eliminating the need to remove the animal's fur, we infected SHO mice but found that the growth kinetics of *Mtb* Charge3 were slower in this mouse strain when compared with those observed in CB-17 SCID mice, and specific fluorescent signals were not detected in these mice by *in vivo* imaging up to day 28 after infection (data not shown). The saline-treated SHO mice at this timepoint were in an earlier stage of infection compared with the CB-17 SCID mice at days 12–15, and did not show weight loss, any symptoms of disease or gross changes in the visible appearance of lung tissue at the time when *ex vivo* imaging of lungs was performed. Again, bacterial burden and fluorescent signals obtained from SHO mice correlated, but here a much lower limit of detection was evident, as an average bacterial

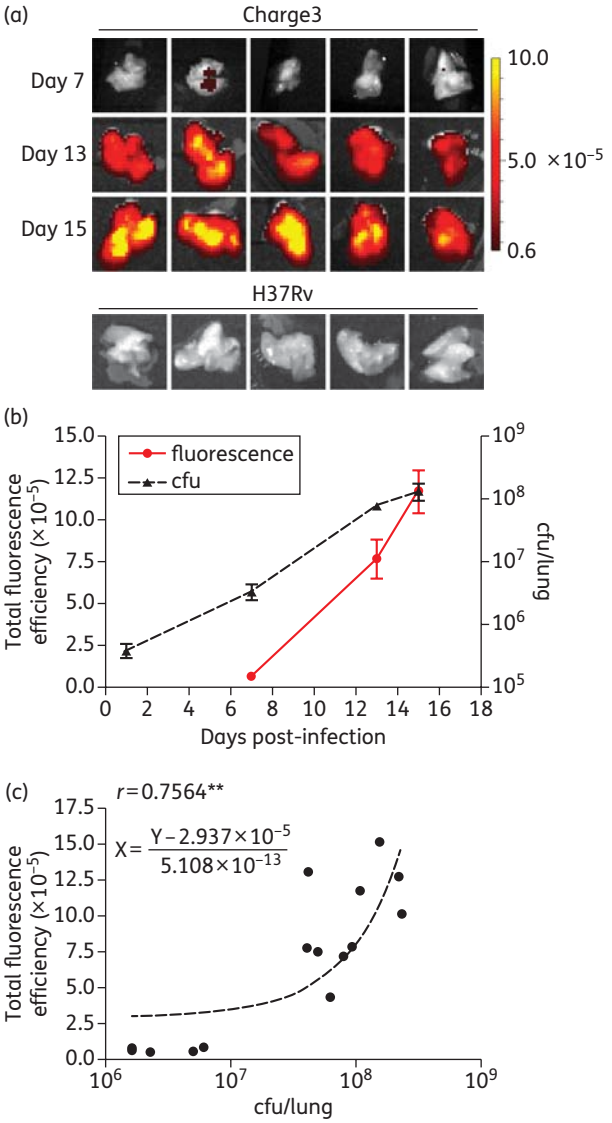

Figure 4. *Ex vivo* fluorescence imaging of lungs harvested from *Mtb* Charge3-infected mice. (a) Groups of CB-17 SCID mice ($n=5$) were infected intranasally with *Mtb* Charge3 or H37Rv WT, then animals were killed and lungs aseptically removed at 7, 13 or 15 days after infection as indicated. (b) Fluorescence (red line) was quantified by drawing an ROI over the thoracic area using Living Image software. Fluorescence is shown as efficiency. cfu data (black broken line) are the same data shown in Figure 3, but are included here for comparison. Data are presented as means ± SEM of five individual mice. (c) Correlation of cfu and fluorescence intensity of lungs shown in (a). Each data point represents an individual organ. The number of cfu X for a given fluorescence measurement Y is described by the equation shown, which was obtained from linear regression analysis. Input inocula/mouse: Charge3, 1.7×10^4 cfu; H37Rv, 2×10^3 cfu. *r* is the Pearson correlation coefficient. $^{**}P<0.01$.

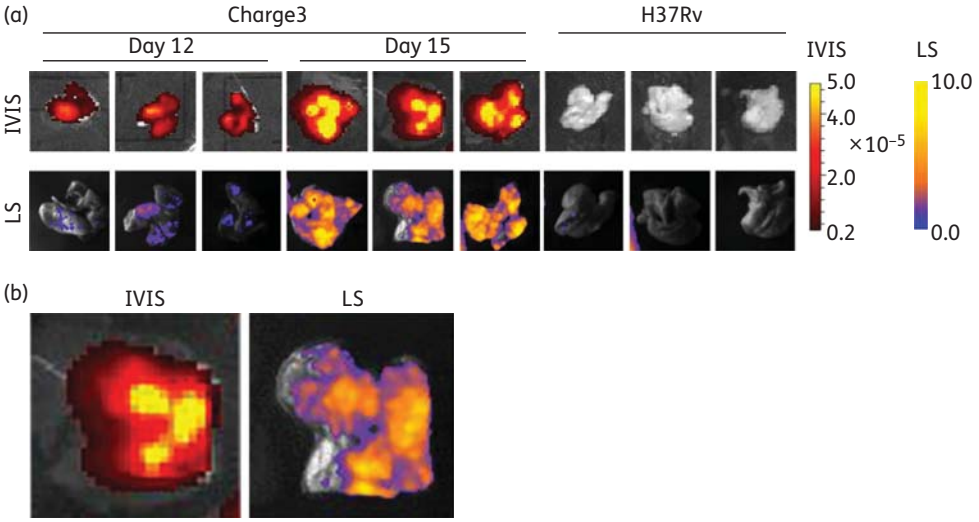

Figure 5. *Ex vivo* imaging of lungs from mice infected with *Mtb* Charge3 or H37Rv, comparing IVIS and LS systems. (a) CB-17 SCID mice were infected with *Mtb* Charge3 ($n=13$) or *Mtb* H37Rv ($n=3$) as an imaging negative control. Mice were killed at 12, 15 or 18 days after infection, and lungs were removed and imaged in the IVIS and LS systems (emission filter 620/40 nm for LS). Representative images were chosen from days 12 and 15. Images from day 12 were chosen as examples of low fluorescence and images from day 15 provide examples of high fluorescence. IVIS images are shown in the top row, with LS images of the same lungs shown underneath. (b) Enlarged copy of images taken from day 15. Fluorescence is presented as efficiency or normalized fluorescence for the IVIS system and LS system, respectively. Input inocula/mouse: Charge3, 4.8×10^4 cfu; H37Rv, 2.3×10^4 cfu.

burden of 2×10^5 cfu/lung on day 19 could be readily detected in both imaging systems, and the calculated detection limits are 5.90×10^4 cfu/lung for the IVIS system and 7.51×10^4 cfu/lung for the LS system. Taking into consideration both the images obtained and the calculated detection limits, and allowing a margin for error, we estimate that both imaging systems are in practice capable of detecting $1-2\times10^5$ cfu/lung, which, however, is reduced in CB-17 SCID mice. The reason for this difference is as yet unclear. One could speculate that, due to the advanced stage of the infection in CB-17 SCID mice, the amount of FP produced by *Mtb* was declining, or that lung inflammation changed the physical properties of the tissue, thereby reducing tissue penetration and the detectable amount of light emitted from bacteria in this organ. Although the plasmid from which the FP is expressed is retained throughout the course of the infection, it is not possible to determine the amount of fluorescence emanating from individual bacteria at the time of imaging using a cfu assay. In our opinion, the SHO mouse is better suited for the TB experiments proposed here due to the slower infection dynamics and no macroscopically visible changes in lung morphology at days 9 and 19 after infection.

All experiments in this study were performed using immunodeficient animals. Whilst detection of *Mtb* fluorescent reporter strains in immune-competent mice using *in vivo* imaging will be challenging due to lower bacterial loads, we expect that our *ex vivo* imaging approach in combination with a high-dose infection and early treatment may also be employed for drug efficacy testing under immune pressure. The assay proposed here is aimed at fast, preliminary assessment of new anti-tuberculosis compounds. Gross pathological changes of lung tissue which are only occurring later in infection are unlikely to influence detection limits significantly. The detection limits we report here are determined by variables of the experimental set-up, such as the sensitivity of currently available CCD cameras and brightness and wavelength of FPs. In future, the development of more sensitive hardware and detection methods and new, bright near-infrared FPs will surely improve on the current detection limits.[30,31]

When comparing the IVIS and LS systems, no difference in sensitivity was found. However, spatial resolution of the fluorescent signal was superior in the LS system compared with the IVIS system. This could facilitate more detailed localization of mycobacteria within the lung tissue, e.g. to determine where bacteria remain in the lung after antibiotic treatment or from where samples should be taken for follow-up studies by microscopy. Other differences between the two systems include ease of use, image collection time per animal and flexibility of the hardware set-up. With its commercial nature, the IVIS system is very user friendly and the software is intuitive, offering simple and time-efficient experimental set-up and operation; however, the hardware set-up has limited flexibility. In contrast, the LS system is custom-built, making it slightly more difficult to use, but its flexible set-up, including laser lines and emission filters, can be freely adjusted and optimized according to the user's requirements. In essence, the IVIS system is ideal for quick acquisition of low-resolution images, whilst the LS system is capable of producing more detailed images but with greater time expenditure.

To develop an efficient assay to test new antibiotics *in vivo*, we adopted an infection model recently developed by Rullas *et al.*,[32] in which antibiotic treatment of mice is initiated 1 day after infection and the effect assessed 8 days later. In that study, moxifloxacin in particular gave very reproducible results and was therefore used here to validate our imaging approach. Indeed, after administering only seven daily doses of the drug,

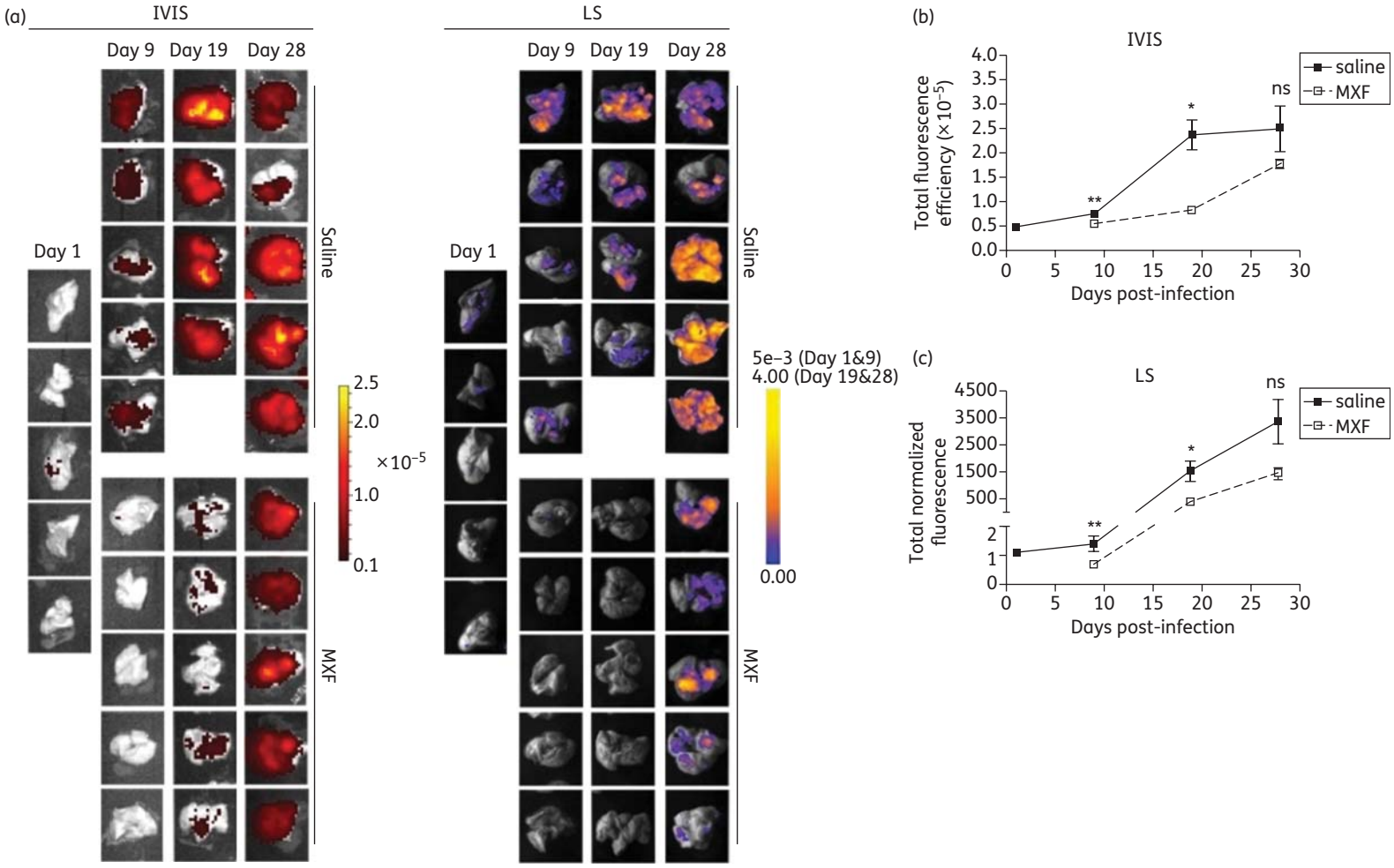

Figure 6. *Ex vivo* imaging of lungs from SHO mice infected with *Mtb* Charge3 and treated with moxifloxacin or saline. (a) Groups of SHO mice ($n=5$) were infected intranasally with *Mtb* Charge3 or H37Rv and given seven daily doses of either saline or moxifloxacin by oral gavage on days 1–7 after infection, and lungs were aseptically removed at 1, 9, 19 or 28 days after infection. Lungs were then imaged in the IVIS and LS systems. Images acquired with the IVIS system are shown on the left and images of the same lungs acquired with the LS system are shown on the right. Fluorescence is presented as efficiency or normalized fluorescence for the IVIS system and LS system, respectively. Note that different scales were used for the LS images on days 1 and 9 and days 19 and 28. (b) and (c) Fluorescence was quantified over time by ROI analysis using Living Image or Matlab software. Data are presented as means ± SEM of individual lungs shown in (a) (saline, filled squares; moxifloxacin, open squares). Input inocula/mouse: Charge3, H37Rv, 3.1×10^3 cfu. $^{**}P<0.01$; $^{*}P<0.05$; ns (not significant) $P>0.05$.

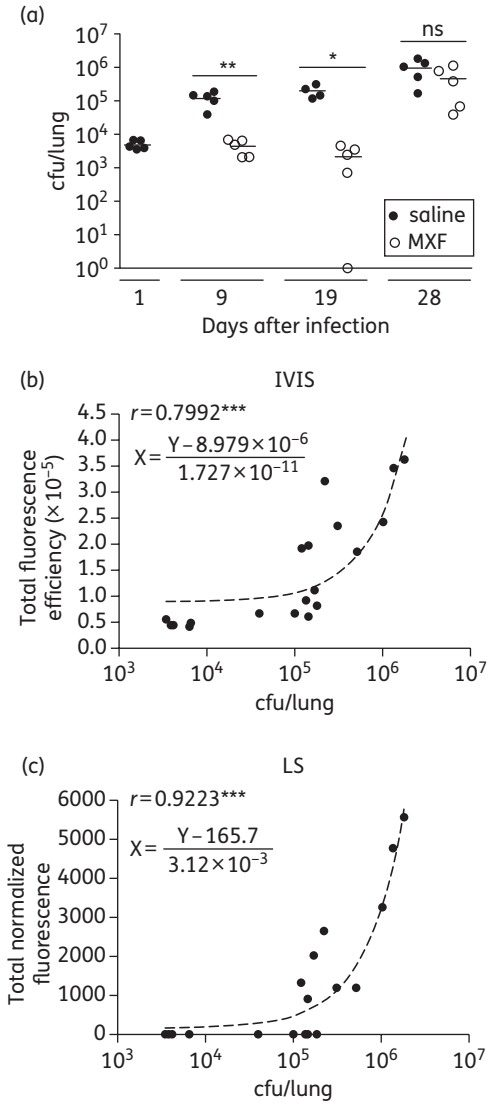

Figure 7. Bacterial burden of lungs from SHO mice infected with *Mtb* Charge3 and treated with moxifloxacin or saline. (a) Lungs of mice from Figure 6 were assayed for bacterial burden at different timepoints after treatment with saline (filled circles) or moxifloxacin (open circles) as indicated. Each data point represents an individual organ and horizontal lines represent the means. (b) and (c) Correlation of cfu in lungs of saline-treated mice to fluorescence measurements of lungs *ex vivo* using the IVIS or LS system. Each data point represents an individual organ. The number of cfu X for a given fluorescence measurement Y is described by the equations shown, which were obtained from linear regression analysis. *r* is the Pearson correlation coefficient. ***$P<0.001$; **$P<0.01$; *$P<0.05$; ns (not significant) $P>0.05$.

we found a significant difference in fluorescence between lungs from saline- and moxifloxacin-treated mice on days 9 and 19 after infection using both the IVIS and the LS system. The difference between the treated and control groups at day 19 was more pronounced than at day 9, and was greater using the LS system compared with the IVIS system (3.99-fold and 2.89-fold, respectively). Notably, the measurements obtained with the IVIS system showed less variation between individual mice within each group. The bacterial load in lungs paralleled the fluorescent signal intensities, with the exception of the moxifloxacin-treated group on day 19 after infection, when the number of bacteria was decreased, whilst the fluorescence was increased compared with day 9. This phenomenon could be explained by the presence of two sub-populations of bacteria, one that still carries the FP and is viable but non-culturable, and another that multiplies while expressing the FP. This could result in the net number of bacteria detected in the cfu assay staying at approximately the same level whilst overall fluorescence increases. As a consequence, the correlation between cfu and fluorescence in the moxifloxacin-treated mice was less stringent and only data from saline-treated mice were included to calculate the detection limits. It has recently been shown for *Salmonella* that a substantial fraction of intracellular bacteria are viable but do not proliferate, a scenario also imaginable for *Mtb*, as it is well known that *Mtb* bacilli can enter a dormant-like state inside the host.[11,33] With the methods used in this study it is not possible to determine the metabolic state of the bacilli *in vivo* or the influence of the metabolic state on fluorescence intensity. We can, however, exclude fluorescence signals from residual FPs after mycobacterial cell death since treatment with bactericidal antibiotics *in vitro* led to rapid loss of fluorescence.[20] Importantly, the significant difference between bacterial numbers determined by cfu assay in moxifloxacin-treated and control mice on days 9 and 19, but not on day 28, mirrors the differences in fluorescence intensities measured and underscores the validity of our imaging assay.

In vivo testing of anti-TB drugs is time-consuming and expensive because most current models are designed to mimic therapy in humans as closely as possible, keeping the initial infectious dose low and initiating treatment 2–4 weeks after infection, when a high bacterial burden in the lung is reached.[34–37] Subsequent treatment is given for several weeks or months, and experiments usually include a relapse group to test whether a drug has sterilizing capability, which further extends the duration of the whole experiment up to 4 months or more. Our assay aims at fast, preliminary *in vivo* assessment of new anti-TB drugs by screening for activity of compounds against replicating bacteria, which could guide subsequent longer term *in vivo* studies, including combinatorial therapy. Other fast assays designed for similar purposes include the use of interferon γ-knockout mice, in which *Mtb* grows rapidly when left untreated, and therefore activity of a new drug can be assessed after only eight treatment doses by the difference in bacterial burden in the treated and untreated groups.[38] However, treatment is only started 18 days after infection following a low-dose *Mtb* infection, and requires a further 4 weeks for completion of the cfu assay. Therefore, the whole assay takes 8 weeks to complete. Our assay indicates after 19 days whether a new drug has anti-TB activity or not. Furthermore, the location of the mycobacteria can be determined, while lengthy cfu assays can be cut out of the testing process. More recently, the use of intravenous infection with *Mycobacterium smegmatis* as a fast-growing model organism for anti-TB drug testing has been suggested,[39] although in this model bacterial load was highest in the spleens, and not lungs, of mice. It therefore does not represent a typical *Mtb* infection, which manifests mainly in the lungs.

To extend the fluorescent *Mtb* reporter system to isolates of more relevance for drug testing, Carroll and Parish have also

produced fluorescent derivatives of the clinical isolate *Mtb* CDC1551 (P. Carroll and T. Parish, unpublished data). Differences in the stability and protein expression of this strain were not observed when compared with *Mtb* H37Rv, suggesting that our system is transferable to clinical and even drug-resistant isolates of *Mtb*.

In summary, we have presented evidence that fluorescent reporter strains of *Mtb* can be visualized by non-invasive optical imaging in living animals at the late stage of an acute, progressive infection in immunodeficient mice. We have also shown that *ex vivo* imaging of target organs such as the lung is a useful and time-efficient method with which to assess bacterial burden and location within the organ with increased sensitivity compared with *in vivo* imaging of whole animals. This *ex vivo* method allowed us to visualize and quantify the effect of antibiotic treatment using either an IVIS system or a custom-built LS system. These imaging assays based on fluorescent *Mtb* reporter strains can now provide novel tools for the analysis of new drugs, in order to speed up the process of identifying promising candidates for the treatment of TB.

Acknowledgements

We would like to thank Robert Gilbert and James Gates from the Biological Services Facility at the London School of Hygiene and Tropical Medicine for their continuous, excellent technical and logistical support, and all members of the Biological Services Facility at the Research Centre Borstel for animal husbandry. We would further like to thank Dr Karsten Stamer for stimulating and helpful discussions and the rest of the Cellular Microbiology group at the Research Centre Borstel for kindly accommodating A. Z. to carry out experiments.

Funding

This work was supported by the Bill and Melinda Gates Foundation TB Drug Accelerator Programme to the Imaging TB consortium (grant number OPP42786).

Transparency declarations

None to declare.

Supplementary data

Figure S1 is available as Supplementary data at *JAC* Online (http://jac.oxfordjournals.org/).

References

1 WHO. *Tuberculosis*. http://www.who.int/mediacentre/factsheets/fs104/en/index.html (23 September 2011, date last accessed).

2 Rowland R, McShane H. Tuberculosis vaccines in clinical trials. *Expert Rev Vaccines* 2011; **10**: 645–58.

3 Colditz GA, Brewer TF, Berkey CS *et al*. Efficacy of BCG vaccine in the prevention of tuberculosis. Meta-analysis of the published literature. *JAMA* 1994; **271**: 698–702.

4 WHO. *Map: Available Data on Anti-TB Drug Resistance, 2010*. http://www.who.int/tb/challenges/mdr/drs_maps_feb2011.pdf (23 September 2011, date last accessed).

5 Dorhoi A, Reece ST, Kaufmann SH. For better or for worse: the immune response against *Mycobacterium tuberculosis* balances pathology and protection. *Immunol Rev* 2011; **240**: 235–51.

6 Russell DG, Cardona PJ, Kim MJ *et al*. Foamy macrophages and the progression of the human tuberculosis granuloma. *Nat Immunol* 2009; **10**: 943–8.

7 Tsai MC, Chakravarty S, Zhu G *et al*. Characterization of the tuberculous granuloma in murine and human lungs: cellular composition and relative tissue oxygen tension. *Cell Microbiol* 2006; **8**: 218–32.

8 Orme IM. The mouse as a useful model of tuberculosis. *Tuberculosis (Edinb)* 2003; **83**: 112–5.

9 Harper J, Skerry C, Davis SL *et al*. Mouse model of necrotic tuberculosis granulomas develops hypoxic lesions. *J Infect Dis* 2012; **205**: 595–602.

10 Apt A, Kramnik I. Man and mouse TB: contradictions and solutions. *Tuberculosis (Edinb)* 2009; **89**: 195–8.

11 Ehlers S. Lazy, dynamic or minimally recrudescent? On the elusive nature and location of the *Mycobacterium* responsible for latent tuberculosis. *Infection* 2009; **37**: 87–95.

12 Patel K, Jhamb SS, Singh PP. Models of latent tuberculosis: their salient features, limitations, and development. *J Lab Physicians* 2011; **3**: 75–9.

13 Contag CH, Contag PR, Mullins JI *et al*. Photonic detection of bacterial pathogens in living hosts. *Mol Microbiol* 1995; **18**: 593–603.

14 Wiles S, Robertson BD, Frankel G *et al*. Bioluminescent monitoring of in vivo colonization and clearance dynamics by light-emitting bacteria. *Methods Mol Biol* 2009; **574**: 137–53.

15 Hardy J, Margolis JJ, Contag CH. Induced biliary excretion of *Listeria monocytogenes*. *Infect Immun* 2006; **74**: 1819–27.

16 Zhao M, Yang M, Baranov E *et al*. Spatial-temporal imaging of bacterial infection and antibiotic response in intact animals. *Proc Natl Acad Sci USA* 2001; **98**: 9814–8.

17 Zhao M, Yang M, Li XM *et al*. Tumor-targeting bacterial therapy with amino acid auxotrophs of GFP-expressing *Salmonella typhimurium*. *Proc Natl Acad Sci USA* 2005; **102**: 755–60.

18 Andreu N, Zelmer A, Wiles S. Noninvasive biophotonic imaging for studies of infectious disease. *FEMS Microbiol Rev* 2011; **35**: 360–94.

19 Gordon S, Chung G, Andrew P. The application of bacterial luciferase as a reporter gene in mycobacteria. *Methods Mol Biol* 1998; **101**: 235–43.

20 Carroll P, Schreuder LJ, Muwanguzi-Karugaba J *et al*. Sensitive detection of gene expression in mycobacteria under replicating and non-replicating conditions using optimized far-red reporters. *PLoS One* 2010; **5**: e9823.

21 Deliolanis NC, Kasmieh R, Wurdinger T *et al*. Performance of the red-shifted fluorescent proteins in deep-tissue molecular imaging applications. *J Biomed Opt* 2008; **13**: 044008.

22 O'Gaora P. Expression of genes in mycobacteria. In: Parish T, Stoker N, eds. *Mycobacteria Protocols*. Totowa: Humana Press, 1998; 261–73.

23 Guo XV, Monteleone M, Klotzsche M *et al*. Silencing *Mycobacterium smegmatis* by using tetracycline repressors. *J Bacteriol* 2007; **189**: 4614–23.

24 O'Gaora P. Expression of genes in mycobacteria. In: Parish T, Stoker N, eds. *Mycobacteria Protocols*. Totowa: Humana Press, 1998; 129–44.

25 Rice BW, Cable MD, Nelson MB. In vivo imaging of light-emitting probes. *J Biomed Opt* 2001; **6**: 432–40.

26 Shaner NC, Campbell RE, Steinbach PA *et al*. Improved monomeric red, orange and yellow fluorescent proteins derived from *Discosoma* sp. red fluorescent protein. *Nat Biotechnol* 2004; **22**: 1567–72.

27 Shcherbo D, Murphy CS, Ermakova GV *et al*. Far-red fluorescent tags for protein imaging in living tissues. *Biochem J* 2009; **418**: 567–74.

28 Kong Y, Subbian S, Cirillo SL *et al*. Application of optical imaging to study of extrapulmonary spread by tuberculosis. *Tuberculosis (Edinb)* 2009; **89** Suppl 1: S15–7.

29 Kong Y, Yao H, Ren H *et al*. Imaging tuberculosis with endogenous β-lactamase reporter enzyme fluorescence in live mice. *Proc Natl Acad Sci USA* 2010; **107**: 12239–44.

30 Subach FV, Piatkevich KD, Verkhusha VV. Directed molecular evolution to design advanced red fluorescent proteins. *Nat Methods* 2011; **8**: 1019–26.

31 Shcherbo D, Shemiakina II, Ryabova AV *et al*. Near-infrared fluorescent proteins. *Nat Methods* 2010; **7**: 827–9.

32 Rullas J, Garcia JI, Beltran M *et al*. Fast standardized therapeutic-efficacy assay for drug discovery against tuberculosis. *Antimicrob Agents Chemother* 2010; **54**: 2262–4.

33 Helaine S, Thompson JA, Watson KG *et al*. Dynamics of intracellular bacterial replication at the single cell level. *Proc Natl Acad Sci USA* 2010; **107**: 3746–51.

34 Nuermberger E, Tyagi S, Tasneen R *et al*. Powerful bactericidal and sterilizing activity of a regimen containing PA-824, moxifloxacin, and pyrazinamide in a murine model of tuberculosis. *Antimicrob Agents Chemother* 2008; **52**: 1522–4.

35 Tasneen R, Li SY, Peloquin CA *et al*. Sterilizing activity of novel TMC207- and PA-824-containing regimens in a murine model of tuberculosis. *Antimicrob Agents Chemother* 2011; **55**: 5485–92.

36 Lounis N, Gevers T, Van Den Berg J *et al*. Impact of the interaction of R207910 with rifampin on the treatment of tuberculosis studied in the mouse model. *Antimicrob Agents Chemother* 2008; **52**: 3568–72.

37 Rosenthal IM, Zhang M, Almeida D *et al*. Isoniazid or moxifloxacin in rifapentine-based regimens for experimental tuberculosis? *Am J Respir Crit Care Med* 2008; **178**: 989–93.

38 Lenaerts AJ, Gruppo V, Brooks JV *et al*. Rapid in vivo screening of experimental drugs for tuberculosis using gamma interferon gene-disrupted mice. *Antimicrob Agents Chemother* 2003; **47**: 783–5.

39 Jhamb SS, Singh PP. A short-term model for preliminary screening of potential anti-tubercular compounds. *Scand J Infect Dis* 2009; **41**: 886–9.